SLAC – PUB – 4612
May 1988
(T/E)

MEASUREMENTS OF TRANSVERSE QUASIELASTIC ELECTRON SCATTERING FROM THE DEUTERON AT HIGH MOMENTUM TRANSFERS*

R. G. ARNOLD, D. BENTON,[a] P. BOSTED, L. CLOGHER
G. DECHAMBRIER, A. T. KATRAMATOU, J. LAMBERT,[b] A. LUNG
G. G. PETRATOS, A. RAHBAR, S. E. ROCK, Z. M. SZALATA
The American University, Washington, D.C. 20016

B. DEBEBE, M. FRODYMA, R. S. HICKS, A. HOTTA,[c] G. A. PETERSON
University of Massachusetts, Amherst, Massachusetts 01003

R. A. GEARHART
Stanford Linear Accelerator Center,
Stanford University, Stanford, California 94309

J. ALSTER, J. LICHTENSTADT
Tel Aviv University, Tel Aviv, Israel 69978

and

F. DIETRICH, K. VAN BIBBER
Lawrence Livermore National Laboratory, Livermore, CA 94550

ABSTRACT

Cross sections for 180° inelastic electron scattering from the deuteron were measured from the break-up threshold to beyond the quasielastic peak for incident beam energies of 0.843, 1.020, 1.189, and 1.281 GeV, corresponding to $0.75 \leq Q^2 \leq 2.57$ (GeV/c)^2. The data are in reasonable agreement with nonrelativistic models that include final-state interactions and meson exchange currents. The scaling function $F(y)$ derived from these data is generally in agreement with $F(y)$ obtained from forward angle data at the same Q^2. Values of G_M^n determined from the data near the top of the quasielastic peaks are in good agreement with results from previous experiments.

Submitted to *Physical Review Letters*

*Work supported in part by the Department of Energy, contracts DOE–AC03–76SF00515 (SLAC), W–7405–ENG–48 (LLNL), DE–AC02-76ER–02853 (U. Mass.) and National Science Foundation Grant PHY85–10549 (A.U.).

[a] Present address: Department of Physics, Princeton University, Princeton, NJ 08544

[b] Permanent address: Department of Physics, Georgetown University, Washington, D.C. 20057

[c] Permanent address: School of Physics, Shizuoka University, Shizuoka, 422 Japan.

Inelastic electron scattering from the deuteron, the simplest nuclear system, is of great importance in understanding the nucleon-nucleon interaction. It offers rich grounds for testing detailed calculations that go beyond the Plane-Wave Impulse Approximation (PWIA) by including Final State Interactions (FSI), Meson Exchange Currents (MEC), and Isobar Configurations (IC). Measurements at the top of the quasielastic peak provide good tests of the impulse approximation, since interaction effects are calculated to be small, and thus have been extensively used in extracting the neutron form factors. The high and low momentum sides of the quasielastic peak are the regions where the nuclear structure functions should be most sensitive to the interaction effects, including the role of constituent quarks in the short-range nucleon-nucleon interaction. Of particular value are data at high momentum transfers, where fully relativistic models can be tested.

In this letter new data are presented for transverse (180°) inelastic electron scattering from the deuteron in the quasielastic region. The data extend to higher momentum transfers or cover a larger range of scattered electron energy E' than previous experiments.[1,2] The measurements were made using the Nuclear Physics Injector and the Stanford Linear Accelerator to deliver electron beams of energy E = 0.843, 1.020, 1.189 GeV, and 1.281 GeV in 1.6 μsec long pulses at average currents of 1 to 5 μA. The beams were transported into End Station A (ESA) and through the chicane magnets of a spectrometer system[3] built for 180° electron scattering measurements[4] of the deuteron elastic magnetic form factor $B(Q^2)$. After passing through 10 or 20 cm long liquid deuterium cells, the beams were directed to a beam dump in ESA. Electrons scattered at 180° were momentum analyzed by the electron arm spectrometer and detected in a set of

six multi-wire proportional chambers. A threshold gas Čerenkov and a lead glass shower counter array were used to reject the large flux of pions. Typically, ten spectrometer settings were used to cover the E' range from break-up threshold to the quasielastic peak and into the region where pion production dominates. At each spectrometer setting, measurements were also made using an empty target so that contributions from the thin aluminium endcaps of the liquid deuterium cells could be subtracted. The data were corrected for detector inefficiencies of 3 to 4%, and in about half of the settings for a large trigger inefficiency of 12 to 31%. For a few runs, corrections up to 24% were made for dead-time losses caused by high counting rates. The dependence of the solid angle on relative momentum $\delta E'/E'$ was calculated within the range $\delta E'/E' = \pm 3\%$ using a Monte Carlo program,[5] and verified experimentally to $\pm 2\%$ by a series of measurements in which the central momentum was stepped in small increments. Checks of the absolute solid angle, made by measuring elastic scattering from the proton using hydrogen targets, gave results that agree within 2% with previous backward angle measurements,[6] as reported in Ref. 3. The spectra were radiatively corrected using the procedures described in Ref. 7. A small correction ($< 1.5\%$) was applied to account for finite resolution effects. The total systematic errors ranged from 3.9 to 12.0%.

The radiatively corrected cross sections at each beam energy E are shown as a function of scattered electron energy E' in Fig. 1. The data are in reasonable agreement with the nonrelativistic PWIA calculations of Laget[8] near the quasielastic peaks, but larger than the calculations by up to a factor of 2 at high E' and up to a factor of 1.5 in the dip region between the quasielastic peak and the onset of pion production at low E'. The Laget calculations use the Paris[9]

potential and a nonrelativistic expansion of the interaction operator to terms of order M^{-3}, where M is the nucleon mass. The matrix elements are evaluated in the lab system. Except in the region where pion production dominates, calculations using the PWIA formulas of McGee as modified by Durand[10] are almost indistinguishable from the Laget PWIA curves when the same potential is used. At high E', the McGee–Durand calculations diverge from the data much more when the Bonn[11] potential is used than when the Paris potential is used, showing the great sensitivity to the short-range part of the potentials in this region.

Considerable improvement is provided by the calculations which include FSI and MEC. The model by Laget, which includes real pion production, describes the low E' side of the peaks well, including the dip region. It reproduces the width of the peaks better than the PWIA calculations, but still underestimates the cross sections close to break-up threshold by up to a factor of 1.5. The calculations of Arenhövel[12] also use the Paris potential, and include IC in addition to MEC and FSI. These calculations use a complete nonrelativistic framework (except for the kinematics which are done relativistically), and the matrix elements are evaluated in the final np center-of-mass frame. This model predicts peaks considerably narrower and taller than seen in the data, with the disagreement increasing at large Q^2. The model does not include real pion production, and so should not be compared with the data on the low E' side of the peaks.

To examine the dominance of the quasielastic reaction mechanism further, the data have been transformed to a scaling function $F(y)$ that should be independent of Q^2 and θ at sufficiently high energies. There are several definitions of y and $F(y)$ in current use,[13,14,15] all based on the notion that scaling will hold true when the electrons scatter incoherently from the individual nucleons, and will be

violated when FSI, MEC, or other mechanisms are important. Figure 2 shows the deduced results for two definitions of

$$F(y) = \frac{d^2\sigma}{d\Omega dE'} \frac{K}{\sigma_n(Q^2) + \sigma_p(Q^2)} \quad .$$

Definition I (see Ref. 13) has $K = |\vec{q}|/\sqrt{M^2 + (|\vec{q}| + y)^2}$, where $|\vec{q}|$ is the absolute value of the three-momentum-transfer, and uses an off-shell prescription[16] for the neutron and proton cross sections $\sigma_n(Q^2)$ and $\sigma_p(Q^2)$. Definition II (see Ref. 14) has $K = dE'/dy$ and on-shell values for $\sigma_p(Q^2)$ and $\sigma_n(Q^2)$ which include a recoil factor $(1 + 2E\sin^2(\theta/2)/M)^{-1}$. In both cases we used the nucleon form factors given in Ref. 10 and the definition of y that solves

$$E + M_d = E' + \sqrt{M^2 + y^2} + \sqrt{M^2 + (y + |\vec{q}|)^2} \quad ,$$

where M_d is the deuteron mass. These definitions were chosen in preference to others because they have the desirable property that the $F(y)$ derived from both the PWIA and full calculations of Laget are independent of electron scattering angle θ at fixed Q^2 and y. In addition, the PWIA calculations scale (independent of Q^2 at fixed y) near the quasielastic peak ($-0.2 \leq y \leq 0.05$) for both calculations. These PWIA calculations also scale in our Q^2 range for $y < -0.2$ GeV/c in Definition I, but exhibit substantial scale breaking in Definition II. For this reason, scale breaking can be directly interpreted as the result of deviations from the nonrelativistic PWIA only for Definition I.

It can be seen in Fig. 2 that our data scale well for $-0.2 < y < 0.05$ GeV/c for both definitions of $F(y)$. For $y < -0.2$ GeV/c, substantial scale-breaking can be observed for Definition I, indicating that FSI or other deviations from the

PWIA are important. The full calculations of Laget also show significant scale breaking in this region. The data scale considerably better for Definition II, as do the full Laget calculations. This definition appears to approximately compensate for the effects of FSI and MEC, and can therefore be used as a convenient way to parametrize data over a large kinematic range.

Also shown in Fig. 2 are data[17,18] obtained at $\theta = 8°$ and $10°$ in the same Q^2 region as the 180° data. Except for $y \leq -0.4$ GeV/c, the $F(y)$ for both the forward and backward angle data are in good agreement. For large negative y, the forward angle $F(y)$ tend to be larger than the backward angle $F(y)$. This trend is not predicted by the full calculations of either Laget or Arenhövel.

In order to examine scale breaking further, in Fig. 3 we have plotted the ratio of experimental cross sections to the McGee–Durand PWIA model (using the Paris wave function) in five different y regions. It can be seen that the ratios for forward and backward angle are generally in agreement, except for the largest $|y|$, where the forward angle ratios are significantly larger than the backward angle ones. The trend of the ratios is to decrease with increasing Q^2 and, for the three plots with the smallest $|y|$, to flatten out at a value of Q^2 which increases with $|y|$. This trend can also be seen to some extent in the calculations of Laget and Arenhövel, and is most likely due to the decreasing importance of FSI with increasing Q^2. In contrast to the $y = 0$ and $y = -0.1$ bins, the ratio for the $y = -0.2$ bin is considerably larger than unity in the region where it is independent of Q^2. This could be ascribed to a lack of high momentum components in the model for the deuteron wave function, or on the influence of objects not included in the model, such as six-quark states. Relativistic corrections could also be of importance.

Historically, quasielastic electron scattering from the deuteron has been used to extract the neutron elastic form factors. We have fitted the McGee–Durand PWIA model to our data close to the quasielastic peak to find values for the neutron magnetic form factor G_M^n in a manner similar to that described in Ref. 18. The contribution of real pion production was subtracted from the data before the fitting was done, using the calculation of Laget.[8] As shown in Fig. 4, the results are in good agreement with both the dipole model $G_D = \mu_N/(1+Q^2/0.71)^2$ and with previous data.[2] The errors on G_M^n are dominated by uncertainties in the normalization of the experimental cross sections, uncertainties due to possible deviations from the PWIA, and the choice of deuteron wave function.

In summary, we have measured 180° cross sections for $d(e,e')$ which fall by over three orders of magnitude between the quasielastic peak and break-up threshold. The results are generally in agreement with a nonrelativistic model that includes MEC and FSI. Detailed agreement has yet to be achieved near break-up threshold, where the effects of FSI, MEC, IC, and the choice of deuteron potential are found to be of increasing importance. Further work using relativistic models and a better knowledge of the short-range nucleon-nucleon interaction will be needed to fully describe the data in this region.

We would like to acknowledge the support of J. Davis, R. Eisele, C. Hudspeth, J. Mark, J. Nicol, R. Miller, L. Otts, and the rest of the SLAC staff.

REFERENCES

1. B. Parker *et al.*, Phys. Rev. C **34**, 2354 (1986); B. Quinn *et al.*, accepted in Phys. Rev. C.
2. W. Bartel *et al.*, Nucl. Phys. B **58**, 429 (1973); K. M. Hanson *et al.*, Phys. Rev. D **8**, 753 (1973); A. S. Esaulov *et al.*, Yad. Fiz 45, 410 (1987).
3. G. G. Petratos, SLAC Report No. SLAC–NPAS–TN–86–7, 1986; A. T. Katramatou *et al.*, SLAC–PUB–4419, 1987, accepted for publication in Nucl. Instrum. Meth.
4. R. G. Arnold *et al.*, Phys. Rev. Lett. **58**, 1723 (1987).
5. A. T. Katramatou, SLAC Report No. SLAC–NPAS–TN–86–8, 1986.
6. L. E. Price *et al.*, Phys. Rev. D **4**, 45 (1971).
7. Y. S. Tsai, SLAC Report No. SLAC–PUB–848, 1971; L. W. Mo and Y. S. Tsai, Rev. Mod. Phys. **41**, 205 (1969).
8. J. M. Laget, Can. J. Phys. **62**, 1046 (1984); J. M. Laget, Phys. Lett. **199B**, 493 (1987), and private communication.
9. M. Lacombe *et al.*, Phys. Lett. **101B**, 139 (1981).
10. I. J. McGee, Phys. Rev. **161**, 1640 (1967) and L. Durand, Phys. Rev. **123**, 1393 (1961) as presented in W. Bartel *et al.*, Nucl. Phys. B **58**, 429 (1973). We used the dipole formula for G_E^p, G_M^p, and G_M^n, and $G_E^n = -Q^2 G_M^n / 4M^2$.
11. R. Machleidt, K. Holinde, and C. Elster, Phys. Rep. **149**, 1 (1987).
12. H. Arenhövel, Nucl. Phys. A **393**, 385 (1983), and private communication.
13. C. Ciofi degli Atti *et al.*, Nucl. Phys. A **463**, 127 (1987).
14. P. E. Bosted *et al.*, Phys. Rev. Lett. **49**, 1380 (1982).

15. G. B. West, Phys. Rep. **18C**, 263 (1975); S. A. Gurvitz and A. S. Rinat, Phys. Rev. C **35**, 696 (1987).

16. A. L. Dieperink *et al.*, Phys. Lett. **63B**, 261 (1976).

17. W. P. Schütz *et al.*, Phys. Rev. Lett **38**, 259 (1977) and R. G. Arnold, private communication for revised results.

18. S. Rock *et al.*, Phys. Rev. Lett. **49**, 1139 (1982).

FIGURE CAPTIONS

1. Cross section for $d(e,e')$ as a function of scattered electron energy E' for four values of the incident energy E. The error bars include statistical and systematic uncertainties. The dotted curves are the PWIA calculations of Laget (Ref. 8) using the Paris potential. The short dashed curves use the PWIA formula of McGee–Durand (Ref. 10) with the Bonn potential, and are indistinguishable from the dotted curves except at high E'. The solid (long dashed) curves are the full calculations of Laget (Arenhövel, Ref. 12) using the Paris potential.

2. Values of $F(y)$ from this 180° experiment (solid squares) and from experiments at forward angles (open circles, Refs. 17 and 18), for two definitions of $F(y)$ (see text). The error bars include statistical and systematic uncertainties. The solid curves represent the full calculations of Laget (Ref. 8) for the four beam energies of this experiment.

3. Ratios of experimental cross sections to the PWIA model of McGee–Durand (Ref. 10) for five values of the scaling variable y. Shown are data from this 180° experiment (solid circles), backward angle data from Ref. 1 (crosses), and forward angle data from Refs. 1, 17, and 18 (open circles). The solid (dashed) curves are the full 180° calculations of Laget (Arenhövel).

4. Values of G_M^n/G_D for this experiment (solid circles) and previous data (Ref. 2, open circles), where $G_D = \mu_N/(1+Q^2/0.71)^2$ is the dipole model. The errors include both statistical and systematic errors added in quadrature.

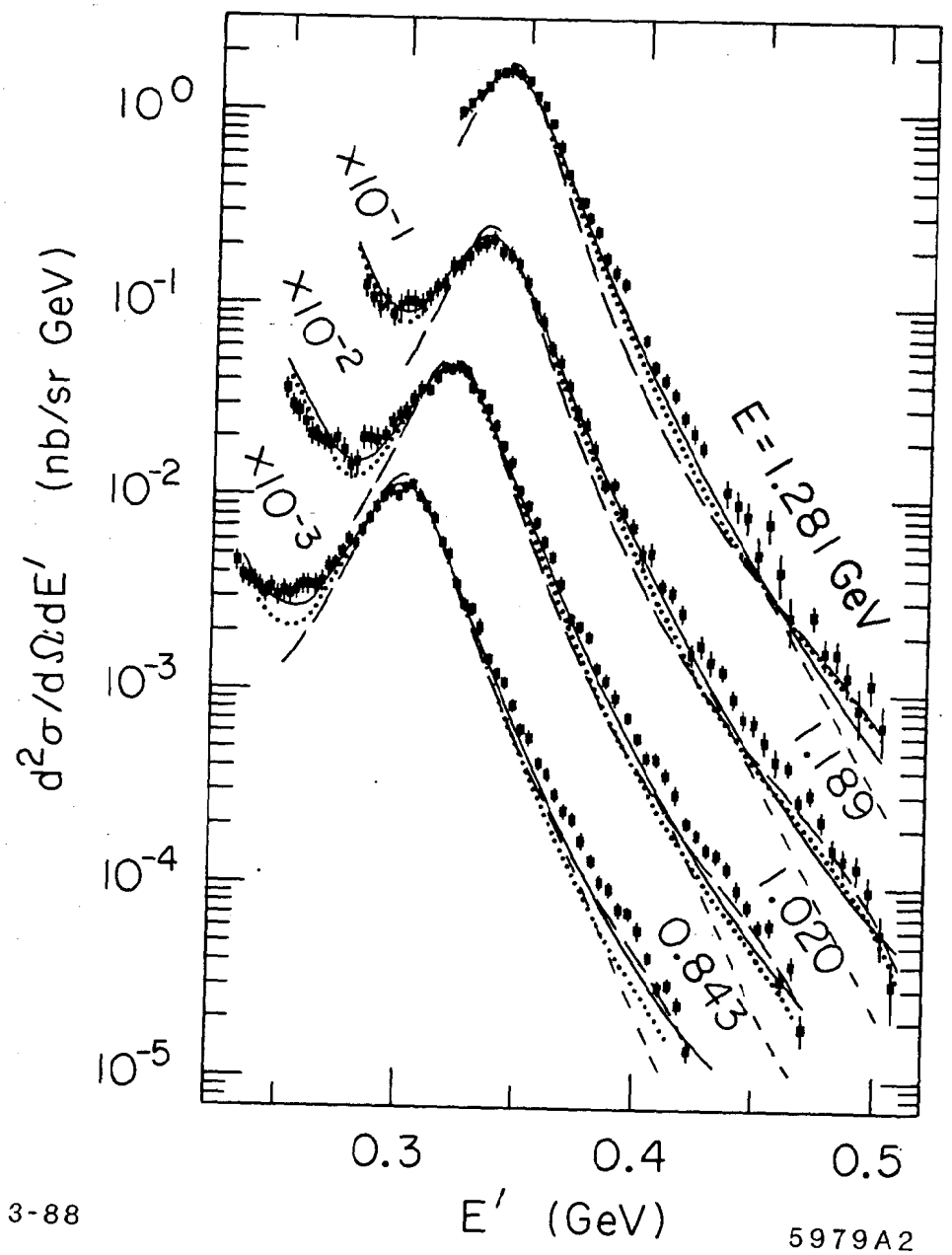
10^0
10^{-1}
10^{-2}
10^{-3}
10^{-4}
10^{-5}
$d^2\sigma/d\Omega dE'$ (nb/sr GeV)
×10⁻¹
×10⁻²
×10⁻³
E=1.281 GeV
1.189
1.020
0.843
0.3
0.4
0.5
E′ (GeV)
3-88
5979A2

Fig. 1

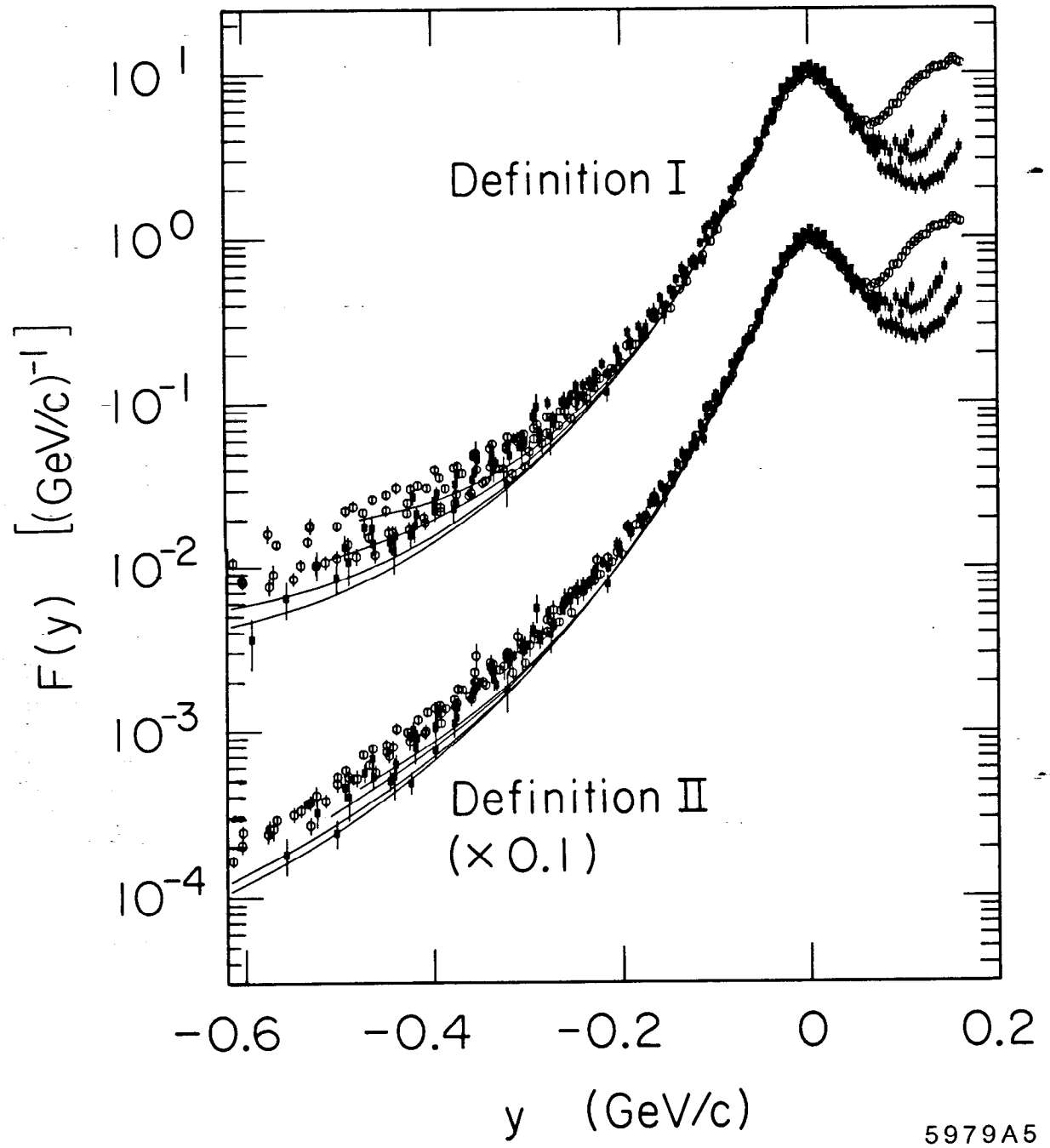
Definition I
Definition II
(× 0.1)
F(y) [(GeV/c)⁻¹]
y (GeV/c)
10¹
10⁰
10⁻¹
10⁻²
10⁻³
10⁻⁴
-0.6
-0.4
-0.2
0
0.2
5979A5

Fig. 2

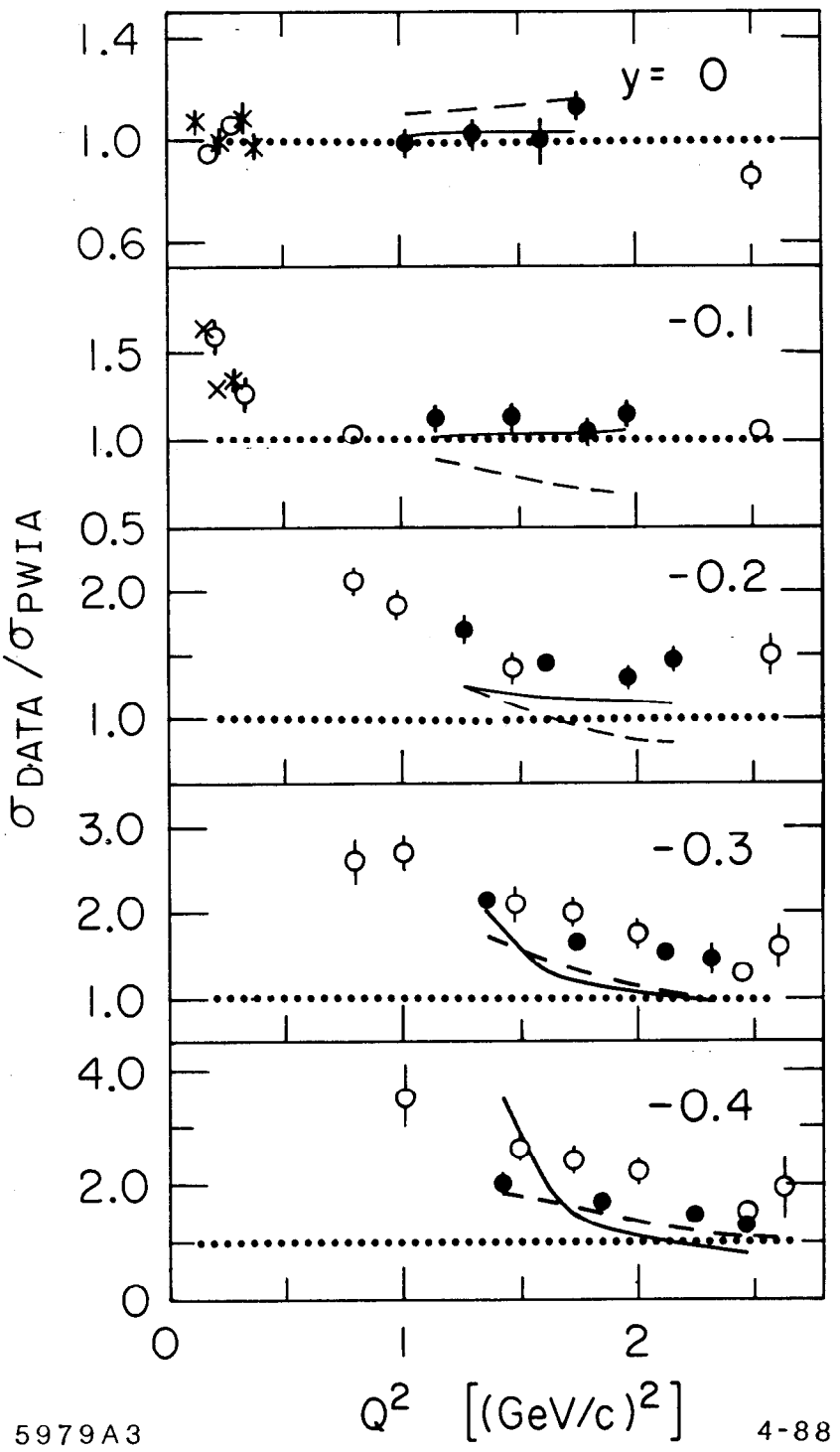

Fig. 3

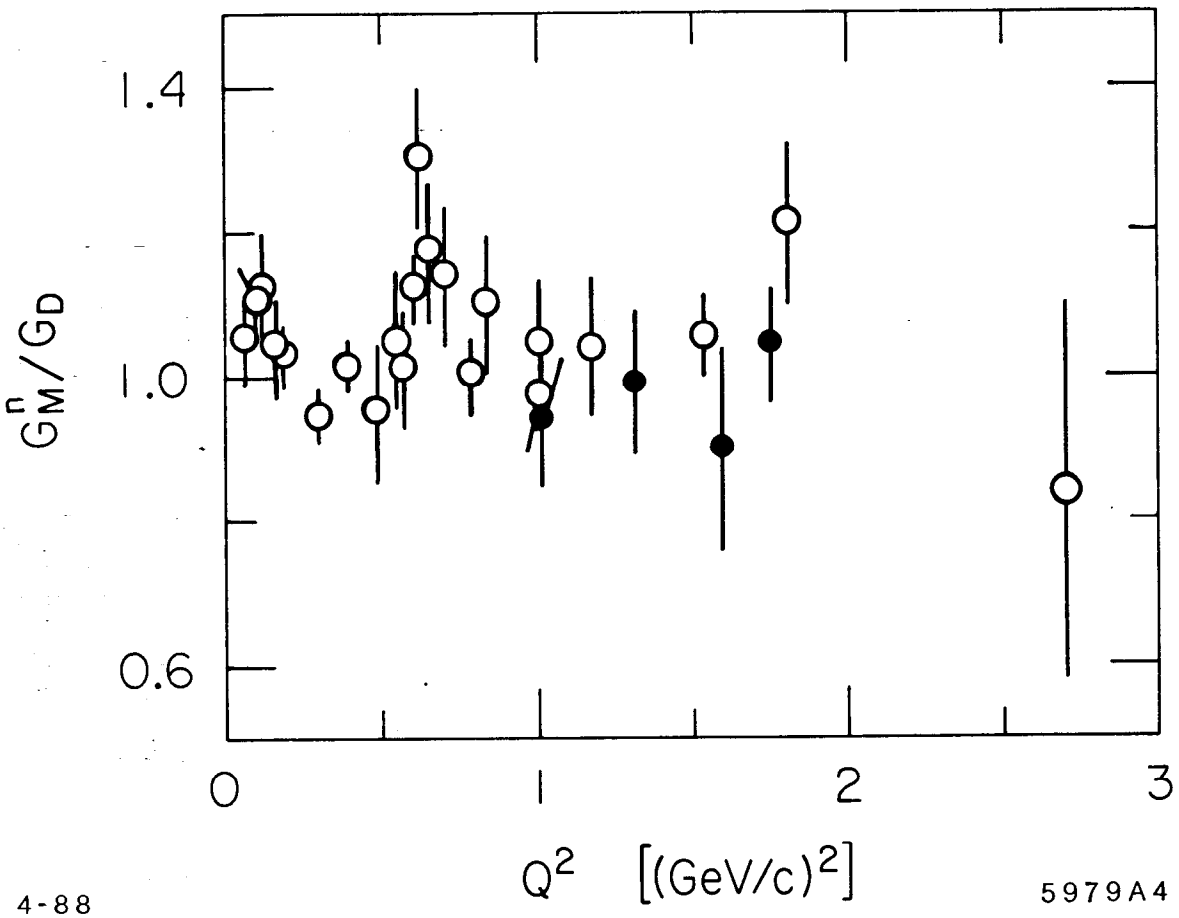

Fig. 4